Probing the influence of channel coupling on the photoelectron angular distribution for the photodetachment from Cu^-

G. Aravind,[1] N. Bhargava Ram,[1] A. K. Gupta,[2] and E. Krishnakumar[1,*]
[1]*Tata Institute of Fundamental Research, Homi Bhaba Road, Mumbai 400 005, India*
[2]*Bhabha Atomic Research Centre, Mumbai 400 005, India*
(Received 27 December 2008; published 15 April 2009)

The electron-correlation effects largely determine the structure and dynamics of anions. Theoretical calculations in the literature indicate the influence of electron correlations on the absolute photodetachment cross section for Cu^-, for photon energies above 3.5 eV, but has not been confirmed experimentally. In the present work we probe the influence of channel coupling on the photoelectron angular distributions for photon energies above 3.5 eV. A velocity map imaging spectrometer was tested and employed in this experiment. The experimental results for the asymmetry parameter show no deviation from the single-electron model. The results indicate no significant influence of the channel-coupling effect on the photoelectron angular distribution in the photon energy range of 3.46–4.6 eV.

DOI: 10.1103/PhysRevA.79.043411 PACS number(s): 32.80.Gc, 33.80.Eh, 32.80.Fb, 33.60.+q

I. INTRODUCTION

The exotic properties of anions and the vital role they play in a variety of phenomena relevant to the plasmas, biological systems, atmosphere of earth and celestial objects, surface dynamics, and many other fields motivate detailed study of their electronic structure and dynamics. Anions are ideal systems to understand the electron-electron correlation effects, which are rather formidable to model [1]. Electron correlations critically determine most of the unique properties of anions [2,3].

Photodetachment is among the most accurate techniques to probe the structural properties of anions through the study of kinetic energy and angular distribution of the detached "extra" electrons [4–7]. A variety of photodetachment techniques [6] have been developed to address different aspects of anion research. Photodetachment microscopy is presently the most accurate technique employed for measuring the electron affinity of anions [8,9]. The photodetachment cross section and the photoelectron angular distribution (PAD) would be influenced by the electron-correlation effects [10,11] and they provide a great deal of information related to the dynamics of photodetachment process.

The photoelectron angular distribution is characterized by an asymmetry parameter that is usually energy dependent [10]. The final-state interactions in the photodetachment process [12] can be understood through the energy dependence of the asymmetry parameter. The asymmetry parameter near autodetaching resonances could have the signature of spin-orbit interactions, which are otherwise difficult to probe [10,13]. Photoelectron angular distributions are usually well described by the single-electron model (Cooper and Zare) [11,12,14]. In the Cooper-Zare central potential model for photodetachment, the ejection of a p-orbital electron should result in s and d detached electron waves, which would interfere to give a characteristic PAD. An s electron that is getting detached would have an outgoing p wave with β equal to 2. The asymmetry parameter in the Cooper-Zare description is given by [14]

$$\beta = \frac{l(l-1)R_{l-1}^2 + (l+2)(l+1)R_{l+1}^2 - 6l(l+1)R_{l-1}R_{l+1}\cos(\delta_{l+1}-\delta_{l-1})}{(2l+1)[lR_{l-1}^2 + (l+1)R_{l+1}^2]}, \quad (1)$$

where R_{l-1} and R_{l+1} are the radial matrix elements, $\delta_{l+1} - \delta_{l-1}$ is their relative phase, and $-1 \leq \beta \leq 2$.

In this model, the orbital angular momentum of the incoming photon is coupled only to the detaching electron with all interactions involving the neutral core neglected and hence it is also called as the single-electron model. However, electron correlations could be significant near autoionization and autodetachment resonances and could induce "kinks" in the spectral dependency of the asymmetry parameter, which are beyond the scope of single-electron model. Fano-type behavior of the vector correlation parameters, such as the β, has been theoretically studied [15], and very recently been observed experimentally near the autoionizing resonances of two-photon-excited iodine atoms [16]. There has also been experimental observation of the deviation of the angular distribution in the photoionization of krypton [13]. In the single-electron model, the s electron from krypton will detach as p wave and the asymmetry parameter for the PAD is equal to 2, which does not vary with the photon energy.

*ekkumar@tifr.res.in

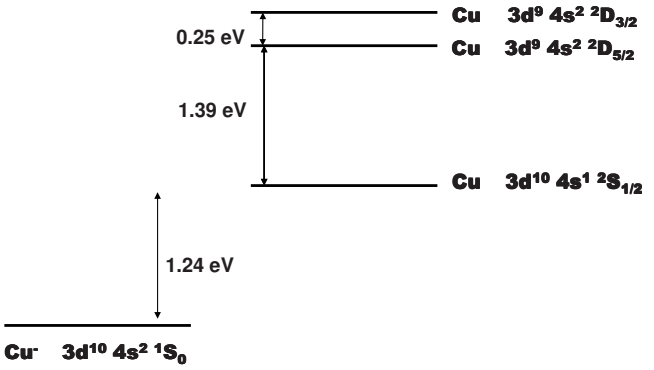

FIG. 1. Energy-level diagram for Cu and Cu^- [19].

Whitfield *et al.* [13] recently observed finite deviation from the value $\beta=2$ near autoionizing resonances of Kr and attributed it to the spin-orbit interactions.

While there have been theoretical predictions [17] for the deviation in the value of β from the single-electron model for photodetachment processes too, to the best of our knowledge, there is no experimental probe for the same. Significant electron correlations in either the initial bound state or the final continuum state would deviate the asymmetry parameter from the predictions of the Cooper-Zare model. Electron correlations in the continuum state are called "channel coupling." Remarkable deviations in the asymmetry parameter can be a convenient probe to autodetachment resonance. It is important to experimentally probe such a deviation from the single-electron model in anions whose electronic structure and dynamics are largely determined by the electron correlations. In the present work we attempt to probe the deviation from the single-electron model in the case of photodetachment of Cu^-. Scheibner and Hazi [18] predicted the effects of channel coupling on the absolute cross section of photodetachment from Cu^-, for photon energies above 3.4 eV. Figure 1 shows the energy-level diagram for Cu and Cu^- [19]. Scheibner and Hazi [18] took a high degree of electron correlations into account in their theoretical calculation for the photodetachment cross section. Their results match well with the experimental data of Balling *et al.* [20] for three photon energies in the range of 1.5–3 eV, for which Balling *et al.* did absolute cross section measurements. The calculated photodetachment cross section [18] shows increase in photon energy above 3.5 eV and is attributed to the channel coupling as the $(3d^9 4s^2)$ doublet D becomes energetically open. There is no experimental probe to the predicted channel-coupling effects on the absolute cross section, which is expected for $h\nu \geq 3.5$ eV. The predicted influence of the channel-coupling effect on the photodetachment cross section would naturally influence the asymmetry parameter, which is a function of the photodetachment cross section. It would be interesting to probe the influence of channel coupling on the photoelectron angular distribution for Cu^- $({}^1S_0+h\nu \rightarrow {}^2S_{1/2}+e^-)$ process. The single-electron model prediction for the asymmetry parameter for the Cu^- $({}^1S_0+h\nu \rightarrow {}^2S_{1/2}+e^-)$ is equal to 2 and is independent of the photon energy, since the outgoing electron is a p wave. Covington *et al.* [21] measured no significant deviation in the value of β of this process for photon energies between 1.92 and 2.71 eV.

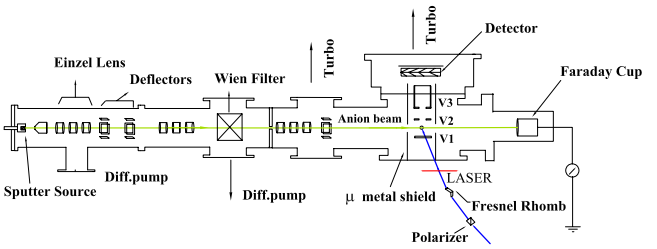

FIG. 2. (Color online) Schematic diagram for the anion photodetachment experimental setup employing the VMI spectrometer.

In this paper, we report the photoelectron angular distribution measurements for Cu^- $({}^1S_0+h\nu \rightarrow {}^2S_{1/2}+e^-)$ process for $h\nu \geq 3.5$ eV. In our earlier experiments we had employed an essentially field-free linear time-of-flight (TOF) photoelectron spectrometer for our angular distribution studies. To probe the deviations from the single-electron model, it is important to have better angular resolution and detection efficiency for low-energy electrons, which are easily perturbed by stray fields. The challenges in detecting low-energy electrons have always restricted the study of energy dependence of photoelectron angular distribution [22–28]. A velocity map imaging (VMI) spectrometer was constructed, tested, and used for the current experiment.

II. EXPERIMENTAL METHOD

The photodetachment experiment on Cu^- was performed using a recently constructed anion photodetachment experimental arrangement [11,12]. The VMI [29], employed for measuring the photoelectron angular distributions and kinetic energies, is based on [30]. Figure 2 shows the complete experimental arrangement. Anions produced from a cesium sputter source were accelerated to about 2.5 keV and mass analyzed using a Wien filter. Three sets of Einzel lenses and X-Y deflectors were employed for efficiently transporting about 40 nA of Cu^- beam over 1.5 m before reaching the interaction region. The anion and the laser beams were made to intersect at right angles. The photoelectrons were ex-

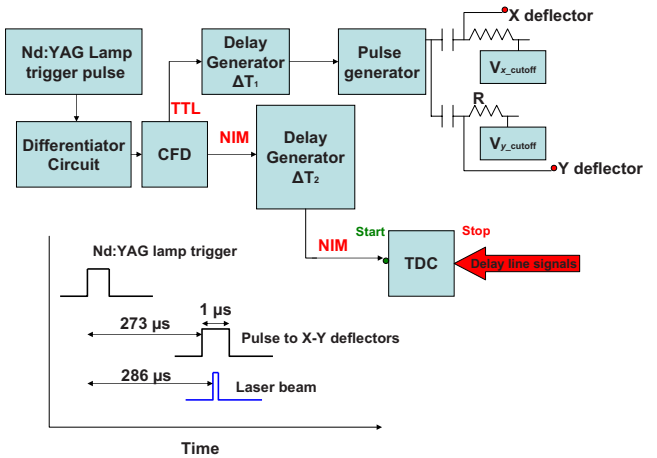

FIG. 3. (Color online) Pulsing scheme for the VMI experiments.

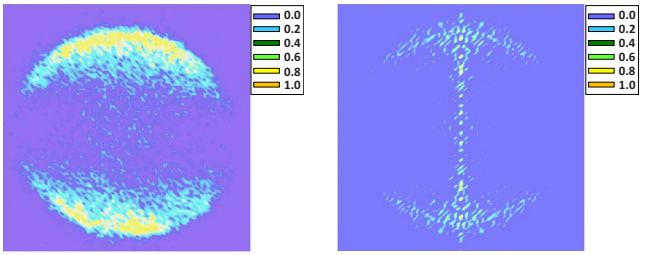

FIG. 4. (Color online) Raw 2D image (left) and the Abel-inverted image (right) for the angular distribution for Cu^- ($^1S_0+h\nu \rightarrow {}^2S_{1/2}+e^-$) process at 532 nm obtained with VMI spectrometer. The central vertical line in the Abel-inverted image is due to artifact from the inversion procedure.

tracted perpendicular to the plane containing these two beams. The interaction region was differentially pumped using turbo molecular pumps to about 2×10^{-8} Torr and was maintained ultraclean.

The VMI spectrometer consists of three electrodes made of oxygen-free high-conductivity (OFHC) copper as shown in Fig. 2. The middle electrode and the flight tube entrance have 26 mm central aperture, and all the three electrodes are separated by 26 mm. The flight tube is 17 cm in length. The middle electrode was grounded and the voltages on the repeller (V_R) and flight tube (V_F) were optimized to achieve the VMI condition. Typically V_R:V_F was about 1:3 for our spectrometer geometry. The entire VMI spectrometer was shielded from the earth's and other stray magnetic fields using two layers of μ-metal sheets as shown in Fig. 2. All materials used in the spectrometer were nonmagnetic. We found it mandatory to coat all the OFHC copper surfaces with colloidal graphite to obtain proper imaging condition. The photoelectrons were detected using a pair of 80-mm-diameter microchannel plates (MCPs) and a delay line hexanode from RoentDeK was employed for recording the position information. The delay line signals were processed by the DLATR-8 RoentDek unit. The output of the DLATR-8 was fed to Lecroy time to digital converter (TDC), which gives the delay-line-signal arrival time with respect to the "start" of the TDC. The TDC was triggered by the Nd-doped yttrium aluminum garnet (YAG) lamp pulse after pulse processing, as shown in Fig. 3.

Custom-made Nd:YAG and Nd:YAG-pumped dye lasers with a repetition rate of 100 Hz were employed in the present experiment. The anion beam was pulsed at 100 Hz repetition rate to minimize the background electrons produced through collision of the anion beam with the residual gas. Figure 3 explains the pulsing scheme that was employed in the experiment. The delay ΔT_1 in pulsing the anion beam (see Fig. 3) was adjusted to achieve temporal overlap of the anion and the laser beam at the interaction region. The linear laser-polarization vector was kept parallel to the detector, which is required to reconstruct the angular distribution from the two-dimensional (2D) projection on the detector.

We used LAMPS [31] acquisition software to compute and display the position of the events obtained from the outputs of the delay line hexanode. The 2D image of the photoelectrons recorded on the detector was Abel inverted [32] to obtain the three-dimensional PAD about the laser-polarization vector. We used the software developed by Dribinski *et al.* [33] for performing the Abel inversion of the raw photoelectron images.

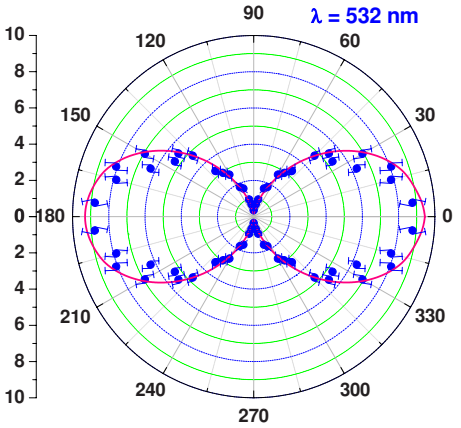

FIG. 5. (Color online) Angular distribution of the photoelectrons for the photodetachment from Cu^- at 532 nm. The solid pink line is a fit to the measured angular distribution. The vertical scale is the photoelectron count rate normalized to the anion current and laser intensity. The statistical error bars for the yield are also shown.

III. RESULTS AND DISCUSSION

The VMI spectrometer was tested for its reliability for PAD measurements by performing photodetachment from Cu^- at 532 nm. Figure 4 shows the raw 2D photoelectron image along with its Abel inversion. A MATLAB code was written to obtain the angular distribution from the Abel-inverted image. The measured PAD was then fitted to the expression $Y(\theta)=a\{1+\beta P_2[\cos(\theta)]\}$ as shown in Fig. 5, where P_2 $[\cos(\theta)]$ is the second-order Legendre polynomial and θ is the angle with respect to the linear polarization vector of the laser. Figure 5 shows the PAD and the β was determined to be 1.94 ± 0.05, which is close to the expected value of 2 at this photon energy value, confirming the reliability of our angular distribution measurement.

The VMI spectrometer was then used to measure the photoelectron angular distribution for Cu^- ($^1S_0+h\nu \rightarrow {}^2S_{1/2}+e^-$) process at 465, 355, 320, and 293.5 nm. We had previously

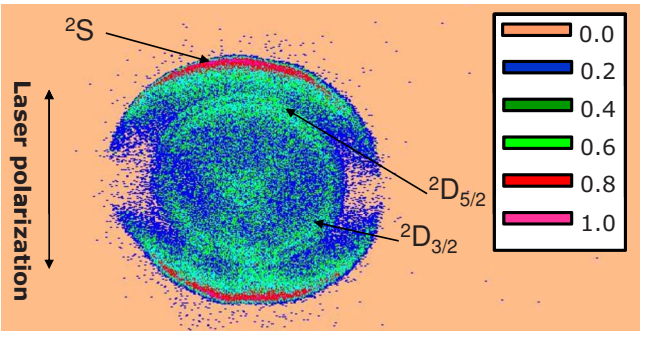

FIG. 6. (Color online) 2D image of photoelectrons from Cu^- photodetachment at 355 nm.

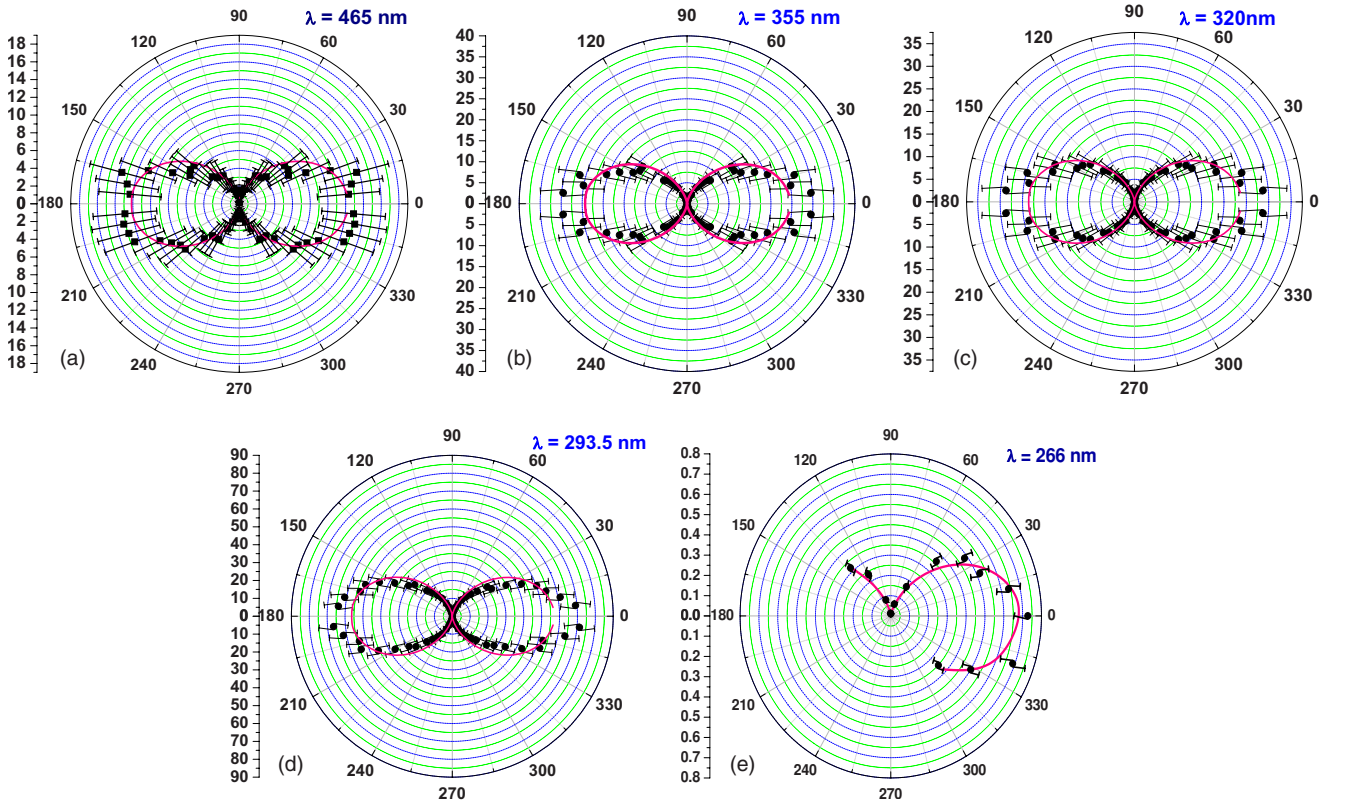

FIG. 7. (Color online) Angular distribution for Cu^- ($^1S_0+h\nu \rightarrow {}^2S_{1/2}+e^-$) process at 465, 355, 320, and 293.5 nm, which were obtained with VMI spectrometer along with PAD at 266 nm which was obtained with the TOF spectrometer. The solid pink line is the fit of the PAD to the expression $Y(\theta)=a\{1+\beta P_2[\cos(\alpha-\phi)]\}$. The vertical scale is the photoelectron count rate normalized to the anion current and laser intensity. The statistical error bars for the yield are also shown.

measured the angular distribution for the same process at 266 and 355 nm using linear TOF spectrometer [11,12]. The 320 nm was the frequency doubled output of the Nd:YAG-pumped (532 nm) sulfurhodomine B, 293.5 nm was the frequency doubled output of Nd:YAG-pumped (532 nm) rhodamine 6G, and 465 nm was Nd:YAG-pumped (355 nm) coumarin 47. The polarization of the doubled dye laser outputs for 532 and 355 nm Nd:YAG pump wavelengths were horizontal and vertical, respectively. We used a half-wave retarder to rotate the vertical polarization to horizontal polarization. The laser-pulse energy was typically 100 μJ per pulse. The VMI voltage conditions for these experiments were ($V_R=-70$ V; $V_F=210$ V) for 465 nm, ($V_R=-100$ V; $V_F=300$ V) for 355 and 320 nm, and ($V_R=-140$ V; $V_F=420$ V) for 293.5 nm.

Figure 6 shows the raw image that was recorded at 355 nm along with the laser-polarization direction. We can clearly see three rings corresponding to the transitions $Cu^-(^1S_0) \rightarrow Cu(^2S_{1/2})$, $Cu^-(^1S_0) \rightarrow Cu(^2D_{5/2})$, and $Cu^-(^1S_0) \rightarrow Cu(^2D_{3/2})$. The radii of these rings calibrate well with the photoelectron energy ($r \propto \sqrt{E}$). As mentioned in Sec. II, the central slice for these images was retrieved using Abel inversion algorithm and the PADs from the inverted images were determined using a MATLAB code. Figure 7 shows the photoelectron angular distributions for this process measured at five wavelengths, including the PAD measurement at 266 nm using the linear TOF. Table I gives the values of β at four wavelengths measured using the VMI spectrometer along with that at 266 nm measured using the linear TOF spectrometer.

Our measurements, with photon energies beyond 3.4 eV, do not show any influence of the channel coupling on the angular distribution, within the experimental uncertainties. There is no theoretical calculation done for the angular distribution for this process and only calculations for photodetachment cross sections are available [18]. Further, there is no experimental confirmation on the increase in the photodetachment cross section due to the influence of channel coupling, which the theory predicts for photon energies beyond 3.4 eV [18]. Balling *et al.* [20] worked with photon energies less than 3.1 eV, where there is no channel coupling pre-

TABLE I. Measured asymmetry parameters for Cu^- ($^1S_0+h\nu \rightarrow {}^2S_{1/2}+e^-$) photodetachment process at 532, 465, 355, 320, 293.5, and 266 nm.

λ (nm)	Photoelectron energy (eV)	β
532	1.08	1.94 (±0.05)
465	1.42	1.97 (+0.03,−0.05)
355	2.24	2 (−0.06)
320	2.62	2 (−0.09)
293.5	2.96	2 (−0.06)
266	3.38	1.95 (+0.05,−0.06)

dicted [18], since the $(3d^9 4s^2)$ doublet D is energetically not open. Thus either there is an insignificant influence of the channel coupling on the angular distribution or there is a need to confirm the presence of the predicted channel coupling [18] by measuring the absolute photodetachment cross sections for $h\nu \geq 3.5$ eV. It is important to experimentally probe the electron-correlation effects on the photodetachment process and we believe that the present work would motivate absolute cross section measurements in the relevant photon energy range.

IV. SUMMARY

A velocity map imaging photoelectron spectrometer was tested and employed to study the photoelectron angular distributions. We probed the influence of channel coupling on the photoelectron angular distribution for Cu^- $(^1S_0 + h\nu \rightarrow {}^2S_{1/2} + e^-)$ process using the VMI spectrometer. Photoelectron angular distributions for this process were measured at 465, 355, 320, and 293.5 nm. These measurements along with our previous measurement at 266 nm, within the experimental uncertainties, do not show any significant deviation from a pure p wave for the outgoing electron. The present results indicate the need to experimentally confirm the predicted behavior of photodetachment cross section for photon energies above 3.4 eV [18]. We believe that the present work would motivate experimental and theoretical investigations on the influence of electron-correlation effect on the photoelectron angular distributions.

ACKNOWLEDGMENTS

We thank Dr. M. Krishnamurthy for useful discussions and providing us with equipment employed in the experiment. We gratefully acknowledge Dr. Ambar Chatterjee and Dr. K. Ramachandran for their assistance in setting up the data-acquisition systems for the current experiment.

[1] Per-Olov Lowdin, Phys. Rev. **97**, 1509 (1955).
[2] T. Andersen, Phys. Rep. **394**, 157 (2004).
[3] V. K. Ivanov, J. Phys. B **32**, R67 (1999).
[4] D. M. Neumark, Phys. Chem. Chem. Phys. **7**, 433 (2005).
[5] D. J. Pegg, Rep. Prog. Phys. **67**, 857 (2004).
[6] T. Andersen, H. K. Haugen, and H. Hotop, J. Phys. Chem. Ref. Data **28**, 1511 (1999).
[7] S. H. Massey, *Negative Ions*, 3rd ed. (Cambridge University, Cambridge, England, 1976).
[8] C. Blondel, C. Delsart, and F. Dulieu, Phys. Rev. Lett. **77**, 3755 (1996).
[9] C. Blondel, W. Chaibi, C. Delsart, and C. Drag, J. Phys. B **39**, 1409 (2006).
[10] S. T. Manson and A. F. Starace, Rev. Mod. Phys. **54**, 389 (1982).
[11] G. Aravind, A. K. Gupta, M. Krishnamurthy, and E. Krishnakumar, Phys. Rev. A **75**, 042714 (2007).
[12] G. Aravind, A. K. Gupta, M. Krishnamurthy, and E. Krishnakumar, Phys. Rev. A **76**, 042714 (2007).
[13] S. B. Whitfield, R. Wehlitz, H. R. Varma, T. Banerjee, P. C. Deshmukh, and S. T. Manson, J. Phys. B **39**, L335 (2006).
[14] J. Cooper and R. N. Zare, J. Chem. Phys. **48**, 942 (1968).
[15] A. N. Grum-Grzhimailo, S. Fritzsche, P. O'Keeffe, and M. Meyer, J. Phys. B **38**, 2545 (2005).
[16] Sandeep Tauro and Kopin Liu, J. Phys. B **41**, 225001 (2008).
[17] Jinhua Xi and Charlotte Froese Fischer, J. Phys. B **32**, 387 (1999).
[18] K. F. Scheibner and A. U. Hazi, Phys. Rev. A **38**, 539 (1988).
[19] R. C. Bilodeau, M. Scheer, and H. K. Haugen, J. Phys. B **31**, 3885 (1998).
[20] P. Balling, C. Brink, T. Andersen, and H. K. Haugen, J. Phys. B **25**, L565 (1992).
[21] A. M. Covington, Srividya S. Duvvuri, E. D. Emmons, R. G. Kraus, W. W. Williams, J. S. Thompson, D. Calabrese, D. L. Carpenter, R. D. Collier, T. J. Kvale, and V. T. Davis, Phys. Rev. A **75**, 022711 (2007).
[22] D. Hanstorp, C. Bengtsson, and D. J. Larson, Phys. Rev. A **40**, 670 (1989); A. M. Covington, D. Calabrese, W. W. Williams, J. S. Thompson, and T. J. Kvale, *ibid.* **56**, 4746 (1997).
[23] J. S. Thompson, D. J. Pegg, R. N. Compton, and G. D. Alton, J. Phys. B **23**, L15 (1990).
[24] Y. Liu, D. J. Pegg, J. S. Thompson, J. Dellwo, and G. D. Alton, J. Phys. B **24**, L1 (1991).
[25] D. Calabrese, A. M. Covington, D. L. Carpenter, J. S. Thompson, T. J. Kvale, and R. L. Collier, J. Phys. B **30**, 4791 (1997).
[26] W. W. Williams, D. L. Carpenter, A. M. Covington, and J. S. Thompson, Phys. Rev. A **59**, 4368 (1999).
[27] V. T. Davis, J. Ashokkumar, and J. S. Thompson, Phys. Rev. A **65**, 024702 (2002).
[28] D. Calabrese, A. M. Covington, W. W. Williams, D. L. Carpenter, J. S. Thompson, and T. J. Kvale, Phys. Rev. A **71**, 042708 (2005).
[29] A. T. J. B. Eppink and D. H. Parker, Rev. Sci. Instrum. **68**, 3477 (1997).
[30] E. Surber, R. Mabbs, and A. Sanov, J. Phys. Chem. A **107**, 8215 (2003).
[31] www.tifr.res.in/~pell/lamps.html
[32] B. J. Whitaker, *Imaging in Molecular Dynamics* (Cambridge University, Press, Cambridge, 2003).
[33] V. Dribinski, A. Ossadtchi, V. A. Mandelshtam, and H. Reisler, Rev. Sci. Instrum. **73**, 2634 (2002).